Effect of unitary impurities in non-STM-types of tunneling in high-T_c superconductors

Jian-Xin Zhu and C. S. Ting
Texas Center for Superconductivity and Department of Physics, University of Houston, Houston, Texas 77204

Chia-Ren Hu
Department of Physics, Texas A& M University, College Station, Texas 77843

Based on an extended Hubbard model, we present calculations of both the local (*i.e.,* single-site) and spatially-averaged differential tunneling conductance in d-wave superconductors containing nonmagnetic impurities in the unitary limit. Our results show that a random distribution of unitary impurities of any concentration can at most give rise to a finite zero-bias conductance (with no peak there) in spatially-averaged non-STM type of tunneling. This is in spite of the fact that local tunneling in the immediate vicinity of an isolated impurity does show a conductance peak at zero bias. We also find that to give rise to even a small zero-bias conductance peak in the spatially-averaged type of tunneling the impurities must form dimers, trimers, etc. along the [110] directions. In addition, we find that the most-recently-observed novel pattern of the tunneling conductance around a single impurity by Pan *et al.* [Nature **403**, 746 (2000)] can be explained in terms of a realistic model of the tunneling configuration which gives rise to the experimental results reported there. The key feature in this model is the blocking effect of the BiO and SrO layers which exist between the tunneling tip and the CuO_2 layer being probed.

PACS numbers: 74.50.+r, 74.62.Dh, 74.80.-g

I. INTRODUCTION

Several years ago, one of us (CRH)[1] showed that the quasi-particle spectrum of a d-wave superconductor (DWSC) contains a special class of excitations — called midgap states (MS's) in that reference — which have essentially zero energy with respect to the Fermi energy, and are bound states with their wave functions localized at the vicinities of various kinds of defects in the system, such as a surface[1] and a grain[2–4] or twin[5] boundary. These MS's form an "essentially dispersionless" branch of elementary excitations, in the sense that their momenta along a flat surface or interface can essentially range from $-k_F$ to k_F (Fermi momentum), and yet with almost no accompanied kinetic energy variation. The existence of surface and interface MS's appears to have already been confirmed by several types of experiments.[6–8] An important question is whether a unitary impurity can also give rise to MS's. The MS's have a topological origin, in the sense that in the semi-classical WKBJ approximation, which makes these states truly midgap, their existence requires the satisfaction of one or more sign conditions only. More precisely, one can describe such a state in terms of one or more (as a linear combination) closed classical orbits, each of which must encounter two Andreev reflections by the pair potential at two different points of the Fermi surface where the pair potential ($\Delta(\vec{k})$) has opposite signs. For each MS formed at a specular surface, only one such closed orbit is involved, so only one sign condition is required.[1] For a MS formed at a flat grain (or twin) boundary, modeled as a planar interface with transmissivity $0 < t < 1$ and different crystal orientations on its two sides, two closed classical orbits are involved, corresponding to the possibility of transmission and reflection at the interface. Thus two sign conditions must be satisfied simultaneously.[4] If a unitary impurity could be represented by a circular hole of a radius much larger than the Fermi wavelength, then quasi-classical argument can be expected to hold, and at least some non-vanishing number of midgap states should exist near its boundary. But when a unitary impurity is of atomic size, such a quasiclassical argument becomes dubious. In fact, if one thinks of scattering by an impurity as a linear combination of infinite number of classical orbits, corresponding to the possibility of scattering by all angles on the Fermi surface, then it would seem that an infinite number of sign conditions would have to be satisfied in order for the impurity to induce some midgap states, corresponding to requiring sign change of the pair potential between any two points on the Fermi surface, which clearly is not satisfied. This argument suggests that midgap states can not form near an impurity, or at least they will not be exactly midgap even in the semiclasscal approximation. However, this argument does not distinguish between a unitary impurity and a non-unitary one. On the other hand, early treatments of a random distribution of unitary impurities in DWSC's, based on the self-consistent t-matrix approximation, have indicated a broad peak at zero energy in the density of states (DOS).[9] (Even earlier similar studies on p-wave SC's also showed such peaks.[10]) Perhaps Balatsky *et al.* are the first to mention within this context that a single *unitary* impurity in a d-wave SC will lead to two zero-energy bound states (per spin), with energies $\pm\epsilon_0$.[11] (Buchholtz and Zwicknagl made a similar statement much earlier for p-wave superconductors.[12]) The t-matrix approximation employed in all of these works, which includes a semiclassical approximation, restores particle-hole symmetry, which is not a very good approximation in high-T_c superconductors (HTSC's). Without this symmetry the energies of

these "MS's" are most-likely not exactly zero. Unlike MS's at surfaces and interfaces, which involve a small number of points on the Fermi surface only, and therefore can easily avoid the gap-node directions, in the case of a state localized around an impurity, all points on the Fermi surface must be involved, including the nodal directions where the gap vanishes. Then for a state whose energy is not exactly zero, its wave function must be able to leak to infinity near the nodal directions. That is, such a state can not be a genuine bound state, and can only be a resonant state. When there is a finite density of impurities, such wave functions should then possess a long-range interaction with each other via the "leakages", leading presumably to a broad "impurity band". The self-consistent t-matrix approximation does not take this point into account properly, and is therefore not satisfactory. (However, see Joynt[13] for an opposite view, except on the assumption of particle-hole symmetry and the validity of neglecting "crossing diagrams" when performing impurity averaging in two dimensions. But we think that neglecting the crossing diagrams is precisely why that approximation can not treat the impurity interaction properly.) A numerical approach has been introduced by Xiang and Wheatley[14] to avoid these shortcomings. For a single unitary impurity and a random distribution of unitary impurities it gave results in good agreement with the t-matrix approximation on the DOS. Numerical solutions of a lattice BCS model with nearest neighbor attraction has also been employed by Onishi *et al.*,[15] who showed that: (i) their exist two essentially-zero-energy states (per spin) localized around an impurity, (ii) their wave functions have long tails in the nodal directions, (iii) as a result such states localized around two impurities separated by a large distance in comparison with the coherence length ξ_0 can still interact with each other, leading to a broad impurity band. Thus the general picture outlined above appears to be confirmed. But Ref. 14 probably also assumed particle-hole symmetry since it plotted the DOS for positive energy only, whereas in Ref. 15 only $\mu = 0$ is considered which has exact particle-hole symmetry. Numerical diagonalization method has also been applied to particle-hole non-symmetric models to study impurity effects, but without addressing the questions raised here. See, for example, Ref. 16. Rather, that work and several other works[17] debated on whether there is localization in the impurity band — a topic which is not our concern here. Instead, we wish to address the roles played by unitary impurities in single-particle tunneling. In particular, it has been noted that MS's formed at surfaces and interfaces of DWSC's can lead to an observable zero-bias conductance peak (ZBCP) in tunneling.[1,4,18–21] Indeed, several recent tunneling experiments performed with[22] STM/S and other tunneling techniques[23] on HTSC single crystals and epitaxial thin films have shown that in ab-plane tunneling a very prominent ZBCP can be observed, especially on {110} surfaces. The observed ZBCP exists continuously for long distances along the surfaces, and the observed tunneling characteristics can be quantitatively fitted by a generalized Blonder-Tinkham-Klapwijk theory[24] which includes the effects of the MS's formed on such surfaces of DWSC's. Assuming that this interpretation is correct, a question one can ask next is: Can unitary impurities be responsible for at least some of the observed ZBCP's? This question is meaningful since ZBCP's have been observed ubiquitously in all kinds of tunneling settings, and some of them may not possess surface and interface MS's. (See Ref. 4 for a review.) Theoretical results reviewed above, although not conclusive, seem to suggest that unitary impurities can also give rise to ZBCP's. But experimental evidence in non-STM/S types of tunneling seem to suggest the contrary. To see that this is the case, one must first exclude ZBCP's observed in ab-plane tunneling, and on tunneling performed on polycrystaline and ceramic samples, since in these cases contributions from the surface and interface MS's can most-likely dominate. (Whereas no MS's can form on a flat {100} surface of a DWSC,[1] surface roughness can reverse this conclusion.[25] Thus we exclude a-axis and $\{n0m\}$-directional tunneling as well, if $n \neq 0$.) One is left with c-axis tunneling on single crystals and epitaxial thin films only. (Nominal c-axis point-contact measurements may actually be seeing some ab-plane tunneling, since the tunneling tips have been pushed into the HTSC samples in these measurements. So they should also be excluded.) Even in the surest c-axis tunneling cases one must still distinguish between STM/S-type tunneling, which can explore the tunneling characteristics in the close vicinity of a single isolated impurity, and the other non-localized tunneling techniques, which see a spatially averaged tunneling characteristics. For the later type, the spectral weight of the impurity contribution must not be too low to be observed, so the impurity concentration must not be too low. It is this kind of tunneling which we are interested in here, since we suspect that once the spectral weight is sufficiently large, the interaction between a random distribution of impurities will also be so large that it still can not give a ZBCP, but only a finite conductance at zero bias, $G(0)$, as a local minimum or even an extra dip. Searching the literature, we find three more recently published papers reporting the STM/S results on the observation of a ZBCP-like feature in the vicinity of an impurity.[26–28] For non-localized tunneling, we find at most a few cases which can weakly suggest that the small ZBCP's observed in them might originate from impurities.[29] (Even in these cases, it is not clear whether MS's could have formed at some exposed CuO_2 edges at the interface with the insulating barrier. The epitaxial films might also have grain boundaries which could host MS's.) Most c-axis tunneling data which exhibit a clear gap feature show a minimum at zero bias, with some showing essentially simple d-wave behavior, with very small $G(0)$,[30] and some showing nearly d-wave behavior but with a finite $G(0)$.[31] Still others show features on both sides of zero bias, giving the impression that there is an extra dip at zero bias.[32] Very few publi-

cations seem to have systematically studied the impurity effects in c-axis tunneling. We find one: Hancotte *et al.*[33] showed that Zn substitution ($\leq 1\%$) in the CuO_2 planes of BSCCO (2212) caused $G(0)$ to markedly increase, accompanied by a reduced gap. Here the spectral weight of impurity effects is clearly large enough, yet not even a trace of a ZBCP was observed.

More recently, the quasiparticle properties around a single impurity have been investigated in more detail in a two dimensional t-J model,[34,35] with a focus on whether the ZBCP observed with STM/S near an impurity is split or not. The purpose of this paper is, on the other hand, to attempt to answer the following precise question: Assuming that HTSC's are DWSC's, and isolated unitary impurities do possess near-zero energy resonant states which can be observed as a ZBCP-like feature by STM/S in the close vicinity of such an impurity, can any concentration of a random distribution of unitary impurities be able to give rise to an observable ZBCP (of any width) in non-STM/S types of tunneling, or there must be some spatial correlation in the impurity distribution before a ZBCP can appear in such types of tunneling? For this purpose we have performed an extensive numerical study. We have introduced the supercell technique so that the finite-size effects from the exact diagonalization can be overcome, and the desired energy resolution can be obtained. This technique has the ability to treat well the impurity of atomic size. Moreover, the band structure effects can be incorporated in a natural way. The results show the conductance behavior is sensitive to the position of the chemical potential within the band and to the impurity configuration at the atomic scale. Our results have indeed confirmed our suspicion that for a simple random distribution of unitary impurities, either their spectral weight is too low for their effects to be observable in non-STM types of tunneling, or their interaction is so strong that only a finite $G(0)$ is obtained as a local minimum rather than a peak, because the impurity band has spread wide, with the center of its contribution to the density-of-states function lower than its two sides. In addition, we find that if only enough number of the unitary impurities form nearest neighbors along the [11] directions in a CuO_2 plane, henceforth called "[11]-directional dimers", then a weak ZBCP can appear in non-STM types of tunneling. (We also find that if enough such impurities form [11]-directional *trimers*, then the ZBCP can be even taller and narrower, but the chance of forming such alignments in an actual sample is probably very low. On the other hand, we think that dimers can probably form with not very low probability.) Furthermore, we have also shown that the most recently observed pattern (by STM/S) of the local tunneling conductance around a single impurity[28] can be explained by taking into account that the STM/S tip in that experiment is separated from the CuO_2 plane under probe by a BiO layer and a SrO layer. Therefore, the tunneling tip can not communicate with the atom directly below it in the CuO_2 plane, due to the blocking effect of the atoms directly above it in the BiO and SrO layers. Rather, we think that the measured "local tunneling conductance" by the tunneling tip on a Cu site in the CuO_2 plane is actually that averaged over a local region around that site, *excluding the contribution from the atom at that site, because of the blocking effect just described*. Using this very reasonable postulate, we find that we can at least semi-quantitatively understand the pattern observed in Ref. 28, including why it peaks at the impurity site, and vanishes at its four nearest neighbor Cu sites, etc.

II. THEORETICAL METHOD

To model decoupled copper-oxygen layers in HTSC's, we consider the single-band extended Hubbard model defined on a two-dimensional square lattice (lattice constant a) with nearest-neighbor hopping, and on-site repulsive and nearest-neighbor attractive interactions.[14] For our purpose, we introduce supercells each with size $N_x a \times N_y a$. We then define the supercell Bloch states labeled by a wave vector $\mathbf{k}$ and a site index $\mathbf{i}$ within the supercell. In the mean field theory, the task becomes to exactly diagonalize the Bogoliubov-de Gennes (BdG) equations:[36]

$$\sum_{\mathbf{j}} \begin{pmatrix} H_{\mathbf{ij}}(\mathbf{k}) & \Delta_{\mathbf{ij}}(\mathbf{k}) \\ \Delta^{\dagger}_{\mathbf{ij}}(\mathbf{k}) & -H_{\mathbf{ij}}(\mathbf{k}) \end{pmatrix} \begin{pmatrix} u^{n,\mathbf{k}}_{\mathbf{j}} \\ v^{n,\mathbf{k}}_{\mathbf{j}} \end{pmatrix} = E_{n,\mathbf{k}} \begin{pmatrix} u^{n,\mathbf{k}}_{\mathbf{i}} \\ v^{n,\mathbf{k}}_{\mathbf{i}} \end{pmatrix} . \tag{1}$$

Here $u^{n,\mathbf{k}}_{\mathbf{i}}$ and $v^{n,\mathbf{k}}_{\mathbf{i}}$ are the Bogoliubov amplitudes corresponding to the eigenvalue $E_{n,\mathbf{k}}$.

$$H_{\mathbf{ij}}(\mathbf{k}) = -te^{i\mathbf{k}\cdot\boldsymbol{\delta}a}\delta_{\mathbf{i}+\boldsymbol{\delta},\mathbf{j}} + (U_{\mathbf{i}} - \mu)\delta_{\mathbf{ij}} , \tag{2}$$

$$\Delta_{\mathbf{ij}} = \Delta_0(\mathbf{i})\delta_{\mathbf{ij}} + \Delta_{\boldsymbol{\delta}}(\mathbf{i})e^{i\mathbf{k}\cdot\boldsymbol{\delta}a}\delta_{\mathbf{i}+\boldsymbol{\delta},\mathbf{j}} , \tag{3}$$

where t is the hopping integral, μ is the chemical potential, $\boldsymbol{\delta} = \pm\hat{\mathbf{x}}, \pm\hat{\mathbf{y}}$ are the unit vectors along the crystalline a and b axes, and $k_{x,y} = 2\pi n_{x,y}/M_{x,y}N_{x,y}a$ with $n_{x,y} = 0, 1, 2, \ldots, M_{x,y} - 1$. $M_{x,y}N_{x,y}a$ is the linear dimension of the whole system, which is assumed to be made of $M = M_x \times M_y$ super-cells. The single-site nonmagnetic impurity scattering is represented by $U_{\mathbf{i}} = U_0 \sum_{\mathbf{i}'\in I}\delta_{\mathbf{i}',\mathbf{i}}$ with the summation over the set of impurity sites. The self-consistent pair potentials are in turn expressed in terms of the wavefunctions $(u_{\mathbf{i}}, v_{\mathbf{i}})$:

$$\Delta_0(\mathbf{i}) = \frac{g_0}{M}\sum_{n,\mathbf{k}} u^{n,\mathbf{k}}_{\mathbf{i}}(v^{n,\mathbf{k}}_{\mathbf{i}})^* \tanh(E_{n,\mathbf{k}}/2k_BT) , \tag{4}$$

$$\Delta_{\boldsymbol{\delta}}(\mathbf{i}) = \frac{g_1}{2M}\sum_{n,\mathbf{k}}[u^{n,\mathbf{k}}_{\mathbf{i}}(v^{n,\mathbf{k}}_{\mathbf{i}+\boldsymbol{\delta}})^* e^{-i\mathbf{k}\cdot\boldsymbol{\delta}a} + u^{n,\mathbf{k}}_{\mathbf{i}+\boldsymbol{\delta}}(v^{n,\mathbf{k}}_{\mathbf{i}})^* e^{i\mathbf{k}\cdot\boldsymbol{\delta}a}] \times \tanh(E_{n,\mathbf{k}}/2k_BT) , \tag{5}$$

where k_B is the Boltzmann constant and T is the absolute temperature. In the case of repulsive on-site ($g_0 < 0$) and nearest-neighbor attractive ($g_1 > 0$) interactions, the d-wave pairing state is favored, the amplitude of which is defined as: $\Delta_d(\mathbf{i}) = [\Delta_{\hat{\mathbf{x}}_a}(\mathbf{i}) + \Delta_{-\hat{\mathbf{x}}_a}(\mathbf{i}) - \Delta_{\hat{\mathbf{x}}_b}(\mathbf{i}) - \Delta_{-\hat{\mathbf{x}}_b}(\mathbf{i})]/4$.

We define the local differential-tunneling-conductance (DTC) by[37]

$$G_{\mathbf{i}}(E) = -\frac{2}{M}\sum_{n,\mathbf{k}}[|u_{\mathbf{i}}^{n,\mathbf{k}}|^2 f'(E_{n,\mathbf{k}} - E) + |v_{\mathbf{i}}^{n,\mathbf{k}}|^2 f'(E_{n,\mathbf{k}} + E)] \,, \quad (6)$$

where the prefactor 2 comes from the two-fold spin degeneracy and $f'(E)$ is the derivative of the Fermi distribution function $f(E) = [\exp(E/k_BT) + 1]^{-1}$. $G_{\mathbf{i}}(E)$ can theoretially be measured by STM experiments. (However, see later for a possible complication when the probed layer and the STM/S tip are separated by other atomic layers.) The spatially-averaged DTC is defined by $G(E) \equiv \sum_{\mathbf{i}} G_{\mathbf{i}}(E)/N_xN_y$, which can essentially be measured in many non-STM/S types of tunneling experiments (planar, ramp, etc.). (But squeezable junctions might measure something in between, depending on the pressure applied.)

III. NUMERICAL RESULTS

In the numerical calculation, we take the supercell size $N_x = N_y = 35$, the number of supercells $M = 6 \times 6$, and the temperature $k_BT = 0.02t$. The lattice sites within one supercell are indexed as (i_x, i_y) with i_x and i_y each ranging from 1 to 35. In addition, we use the bulk value of the order parameter as an input to diagonalize Eq. (1) and the deformation of the order parameter near the impurity is ignored. (This approximation should be quite acceptable for the questions we wish to answer here.) In the bulk system, the d-wave order parameter has the form $\Delta_{\mathbf{k}} = 2\Delta_d(\cos k_x a - \cos k_y a)$, where $k_{x,y}$ are the x- and y-components of the wave vector defined on the whole system. Table I lists the resulting d-wave pair potential Δ_d and coherence length $\xi_0 = \hbar v_F/\pi\Delta_{\max}$ for the chosen values of g_1 and μ, where v_F is the Fermi velocity and $\Delta_{\max} = 4\Delta_d$ is the maximum energy gap. The choice of the maximum energy gap is consistent with the bulk gap structure exhibited in the bulk DOS. In the calculation of Δ_d, an arbitrary negative value of g_0 can be taken.

A. The cases of a single impurity and a small cluster of impurities

The quasiparticle property near a single impurity in a DWSC is complicated, and whether the energy of quasiparticle resonant states is exactly zero (relative to the Fermi energy) or whether the zero (or near-zero) energy states are split is very sensitive to the band structure and the impurity strength. To give a clear answer or clue to this question, we first consider the case of weak or moderately strong impurity. Figure 1 plots the local DTC as a function of bias directly on the single-site impurity (a) and one lattice constant away (b). As shown in Fig. 1, when the impurity scattering is weak ($U_0 = 2.5t$), the local DTC on the impurity site has a peak below the Fermi energy, which is consistent with the earlier study within the continuum theory;[11] while that at the site nearest-neighboring to the impurity has a double peak structure, one above and the other below the Fermi energy. When the impurity scattering becomes stronger ($U_0 = 10t$), the peak on the local DTC on the impurity site is pushed toward the Fermi energy with the amplitude strongly suppressed; nevertheless the double peaks on the local DTC at the nearest-neighbor site converge to each other and the intensity is enhanced. Since $\mu = 0$ in this calculation, the band is globally particle-hole symmetric. Therefore the non-zero energy resonant states shown above originates from the local particle-hole symmetry breaking. Differently, when the impurity scattering goes to the unitary limit, whether there exists the particle-hole symmetry depends on solely on the position of chemical potential within the band.

In all the following discussions, the single-site impurity potential strength is taken to be $U_0 = 100t$, so it is practically in the unitary limit. In Fig. 2 the local DTC is plotted as a function of bias near one single-site impurity located at site $(18, 18)$ for various values of μ but with $g_1 = 2t$ fixed. The bias is normalized to $\Delta_{\max}$. The tunneling point is one lattice constant away from the impurity along the (10) direction, i.e., at (19, 18). As is shown, when $\mu = 0$ where the particle-hole symmetry holds, a sharp zero-bias conductance peak is exhibited. When μ deviates from zero, the line shape of the local DTC becomes asymmetric with respect to the zero energy position. The peak near zero energy is seen to show an incomplete splitting and the height of this peak is decreased. The extent of splitting increases with the deviation of μ from zero. This result is quite different from the case of a {110}-oriented surface, where an un-split zero-energy peak in the local DTC shows up regardless of the position of the chemical potential. The similarity between the result obtained here by solving the extended Hubbard model and the corresponding result we obtained earlier by solving the t-J model[35] indicates that our conclusion about the splitting of the ZBCP is, at least in the mean field level, model independent. Next, we show that when more than one unitary impurities are present in the SC, the local DTC heavily depends on the impurity configuration. In Fig. 3, we plot the local DTC in a DWSC with two and three impurities forming a [11]-directional nearest-neighbor dimer and trimer, respectively, for $g_1 = 2t$ and $\mu = -t$. Without loss of generality, the impurity positions are placed at sites (17,19) and (18,18) for the dimer case, and at sites (17,19), (18,18) and (19,17) for the trimer case. The

measured position is still at site (19,18). As can be seen clearly, the near-zero-energy peaks in the local DTC for the single impurity case are strongly pulled toward zero energy in the dimer case. In the trimer case, the zero-energy peak is even more pronounced. To check this point more seriously, we have also calculated the lowest positive eigenvalues for the system composed of one supercell with one single impurity, and two impurities with different relative positions for $g_1 = 2t$ and $\mu = -t$. We find that a single impurity leads to two near-zero-energy states per spin, one just above and one just below the Fermi energy. The absolute energy corresponding to these two eigenstates is roughly $0.1t$. (It is not zero because there is no particle-hole symmetry in this model study.) But for the two impurities positioned as nearest neighbors of each other along the [11] direction, the lowest positive eigen-energy is only about $0.03t$. If two impurities are positioned as nearest neighbor of each other along the [10] direction, the lowest positive eigenvalue is roughly $0.09t$, which is very close to the value for isolated impurities. In Fig. 4, we have plotted the variation of the lowest positive eigenvalue with the distance between two imputities aligned along the [11] direction. When two impurities are far apart, the lowest positive eigenvalue oscillates between $\sim 0.105t$ and $\sim 0.079t$, around the value $\sim 0.1t$ for isolated impurities, as the distance between the two impurities are increased. This oscillation is a clear indication of the long range interaction between two impurities that we have already discussed. (The long tails of the wave function of a bound state around a unitary impurity in the nodal directions are oscillating in Fermi wavelength, so the sign of the interaction between two impurities can change with distance.) When two impurities form a [11]-directional dimer, they combine to play the role of a very short {11} edge. That is, they drastically enhanced the probability for specular reflection by this edge, so the nearest-to-zero eigen-energies become very close to zero energy. This analysis demonstrates that the closest-to-zero eigen-energies due to the presence of impurities are very sensitive to the short-range correlations in the impurity configuration. Furthermore, we plot in Fig. 5 the number of near-zero eigen-energy states versus the number of impurities aligned consecutively along the [11] direction. In this calculation, each state with its eigenvalue smaller than $0.04t$ is counted as a near-zero-energy state. As the result shows, the number of near-zero-energy states increases almost linearly with the length of a [11]-directional impurity line. We also find that, as the number of impurities is increased, there are more and more states with their eigen-energy approaching zero, which confirms from an alternative aspect that the appearance of the ZBCP in the {110}-oriented DWSC tunnel junctions is independent of the position of μ in the band.

Most recently, Pan *et al.*[28] have performed an STM study on the effect of a single zinc (Zn) impurity atom on the quasiparticle local density of states (LDOS) in BSCCO. Besides revealing the predicted highly localized four-fold quasiparticle cloud around the impurity, the imaging also exhibited a novel distribution of the near-zero-resonant-energy LDOS near the impurity. In contrast to the existing theories, which give a vanishing LDOS directly at the site of the unitary impurity, and vanishing or low values on all atomic sites along the [11] directions and at the (20) and (02) sites, it was observed that the LDOS at the resonance energy has the strongest intensity directly on the Zn site, scattering from which is believed to be in the unitary limit. In addition, the LDOS at the resonance energy has nearly local minima at the four Cu atoms nearest-neighbor to the Zn atom, and has local maxima at the second- and third-nearest-neighbor Cu atoms. The intensity of the LDOS on the second-nearest-neighbor Cu atoms is larger than that on the third-nearest-neighbor Cu atoms. Although this unexpected phenomenon might indicate strong correlation effects, we would rather try to explain it from an alternative point of view. Superconductivity in HTSC's is believed to originate in the CuO_2 plane, and the STM/S tip at low bias is known to be probing such a plane closest to the surface. But the STM tip is also known to be separated from this plane by a BiO layer and a SrO layer. The BiO layer is believed to be semiconducting and the SrO layer, insulating. So low-energy electrons can go through them. However, the hard cores of the atoms surely can block the tunneling current from directly going through them. We therefore postulate that tunneling occurs from the tip to the atoms within a small circular area in the CuO_2 plane directly below the tip, except those atoms blocked in the above sense. In addition, we postulate that the linear dimension of the small circular area is only a little larger than the lattice constant a, because the negative-exponential dependence of the tunneling current on distance implies that we need only include the closest set of atoms that *can* contribute to the tunneling current. (That is, they are not blocked by the atoms in the BiO and SrO layers closer to the surface than the CuO_2 layer being probed.) Then the tip above a given Zn or Cu site in the CuO_2 plane sees only its four nearest-neighbor sites in that plane. Therefore, we propose that the actual measured LDOS at a Zn or Cu site is essentially the sum of the contributions from its four nearest (Cu or Zn)-neighbors. The measured local DTC should then be related to the calculated local DTC by the relation:

$$G_{\mathbf{i}}^{\text{expt.}}(V) = \sum_{\boldsymbol{\delta}} G_{\mathbf{i}+\boldsymbol{\delta}}^{\text{calc.}}(V). \tag{7}$$

In Fig. 6, part (a), the spatial distribution of the calculated bare [*i.e.*, before the transformation given in Eq. (7)] DTC at zero bias is displaced in a three-dimensional plot. It includes the effects of all four near-zero-energy resonant states (two per spin) localized around a unitary impurity.[38] The temperature is assumed to be at $k_BT = 0.02t$ (or $T \simeq 0.1T_c$) in the calculation. The parameter values $g_1 = 1.5t$ and $\mu = -0.4t$ are cho-

sen to obtain a single near-zero-bias conductance peak. These values are not yet optimized, since at the present time we only wish to establish the essential correctness of our idea. In Fig. 6, part (b), a planar "bubble plot" of the same data is given, where the size of each black dot is directly proportional to the calculated bare-DTC at that lattice site. (Our calculation, being tight-binding in nature, gives DTC values only at the lattice sites, unlike the observed data, which gives a continuous variation of the DTC between the atomic sites.) In Fig. 6, parts (c) and (d), similar plots are given for the calculated transformed-DTC based on Eq. (7). It is clear from comparing these plots with Fig. 3(b) and (c) of Ref.[28] that the calculated transformed-DTC-distribution agrees quite well, at least qualitatively, with the measured DTC-distribution at the resonant energy in that reference.

As a crude quantitative comparison between our prediction based on Eq. (7) and the measure data of Pan *et al.*, we have listed in Table II the normalized measured values by Pan *et al.* [based on Fig.4 (a) in Ref.[28]], our normalized calculated bare values, and our normalized calculated transformed values [by using Eq. (7)], of the local DTC at various lattice sites near a Zn impurity [which is defined to be the (00) site], up to the third nearest-neighbor [*i.e.*, the (20) and (02)] sites. Within each row of data, the normalization is such that the largest value becomes unity. (For the first and third rows of data, this occurs at the (00) site, but for the second row of data, this occurs at the (10) and (01) sites, because the calculated bare value of the local DTC at the resonant energy vanishes at the (00) site.) We admit that this comparison is only a very crude one, since our tight-binding result for the DTC distribution, which exists at the Zn and Cu sites only, and not continuously in between them, should, strictly speaking, be compared with some integrated result of the measured local DTC. But in the first row of Table II we have only listed the measured local DTC values right at the Zn and near-by Cu sites, with no integration performed. In fact, we strongly believe that the agreement will be much better if we do perform properly such an integration of the measured data before comparison with our prediction, as may be seen by comparing our prediction given in Fig. 6, part (d), and the Fig. 3(b) of Ref.[28], or the three-dimensional figure on the cover page of the March 2000 issue of Physics Today[39]. This is particularly so with regard to the relative heights of the local DTC measured at the (10) or (01) sites, and those at the (20) and (02) sites. The former is larger than the latter in the data given in the first row of Table II, and in Fig. 4(a) of Ref.[28], where the data in the first row of table II came from. However, since at the moment we have not figured out the proper way to do this integration, we shall leave that to a future publication. (An even better theory should generate a continuous local DTC in a plane, to be directly compared with the measured data, with no integration needed. This possibility will also be looked into later.) In spite of the fact that the comparison presented in Table II is only a very crude one, we believe it still strongly suggests that our idea is essentially correct, although the model clearly can and should be improved, in order to give a local DTC distribution which exists *continuously* in a two-dimensional plane, as has been observed.

B. The case of randomly distributed impurities

In Fig. 7, we have plotted the *spatially averaged* DTC for different concentrations of impurities contained in the DWSC. The parameters chosen are: $g_1 = 2t$ and $\mu = -t$. When the super-cell contains only one impurity, because the spectral weight from the impurities is too small for this density (0.08%) of impurities, only a very small spatially-averaged zero-bias DTC, $G(0)$, appears, without a slight trace of a ZBCP. At this low concentration of impurities, $G(V)$ practically reflects the bulk d-wave DOS. The conductance peak outside the positive maximum energy gap stems from the van Hove singularity. To increase the spectral weight of the impurity contribution to $G(V)$, one needs to increase the density of impurities, in presumably a random distribution. But as shown by the dashed line in Fig. 7, in which the randomly-distributed impurity density has been increased to 1.28%, one still does not obtain an observable ZBCP in spatially-averaged $G(V)$, but only a finite spatially-averaged $G(0)$ as a local minimum. This we think is because the wave functions of the near-zero-energy resonant states around the impurities have tails along the near-nodal directions, the interaction between such states at different impurity positions (especially between those impurities not very far away from each other) is so large that the contributions from these states to the DTC has spread into a wide band with actually lower value at the band center (i.e., zero bias) than at the band edges. This is consistent with the fact that in most c-axis non-STM-types of tunneling experiments, only a finite $G(0)$ is observed, without showing a peak there of any shape and width.

Compared with the single impurity case plotted by the solid line, it is clear that $G(0)$ is enhanced at this much higher density of randomly-distributed impurities, showing that the spectral weight of the impurity contribution at this density of impurities is clearly no longer negligible. Yet no trace of a ZBCP is obtained. On the other hand, we find that at the same concentration of impurities, if a good portion of these impurities form [11]-directional dimers, (with separation $\sqrt{2}a$ between the two impurities in each such dimer,) but still with random orientations, a small observable ZBCP is exhibited in $G(V)$. [See the short-dashed line in Fig. 7], in which 62.5% of the impurities form such dimers. We have also calculated the wavefunction near the two impurities forming such a dimer and found that the wavefunction amplitude is very small along the alignment direction of the two impurities, but has an oscillatory behavior perpendicular to the alignment direction. This highly anisotropic behav-

ior of the wavefunction may have drastically suppressed the interaction between the impurities. The height of the ZBCP depends on the total number of impurities forming such dimers. We also find that if some impurities form [11]-directional *trimers*, the amplitude of the ZBCP can be enhanced even further. But we deem the probability for three impurities to form such a trimer in an actual system is very small, but the assumption that some impurities can form [11]-directional dimers should be reasonable. Thus we propose that this is how impurities can possibly contribute to some of the observed ZBCP's, and why often ZBCP's are not observed in c-axis non-localized tunneling, even in samples which have been deliberately introduced some substantial amount of substitutional non-magnetic zinc (Zn) impurities.[33]

IV. SUMMARY

In summary, we have made detailed calculations of both the local and the spatially-averaged differential tunneling conductance in DWSC's containing nonmagnetic impurities in the unitary limit. Our results show the following: (1) Previously we have shown[35] that the local conductance behavior near zero energy at the sites near a unitary impurity is sensitive to how well the particle-hole symmetry is satisfied, and how large is the error of using a semiclassical WKBJ approximation to treat the problem. Here we have demonstrated that conclusion is model independent. (2) We also find that the conductance behavior is very sensitive to the impurity configuration. For the single-impurity case, a recently obtained LDOS imaging at the resonance energy has been explained in terms of a model where the blocking effect of the atoms in the BiO and SrO layers are taken into account, so that the tunneling tip does not probe the local density of states of the Cu or Zn site directly below it, but rather essentially the sum of those of its four nearest neighbor sites. Furthermore, our study allows us to conclude that unitary impurities can contribute to an observable ZBCP in non-localized tunneling if and only if a substantial number of impurities form [11]-directional dimers, (and trimers, etc.). On the other hand a simple random distribution of unitary impurities either has too low a spectral weight to contribute observably to non-localized tunneling, or their interaction is already so strong that they can only produce a finite value at zero bias in non-localized tunneling conductance without giving a peak there of any shape or width. An ultimate test of this scenario would require: (i) the observation of a ZBCP in STM/S tunneling in the close vicinity of a unitary impurity, (which is already achieved recently); (ii) the non-observation of a ZBCP in non-STM/S types of c-axis tunneling on a single-crystal sample with any concentration of the same type of impurities which are confirmed to not have formed [11]-directional dimers, (or trimers, etc.); and (iii) the appearance of a small ZBCP in the same types of tunneling experiments when the impurity distribution is established to contain such dimers, (or trimers, etc.). Such an ultimate test may be asking too much from the experimentalists, but the fact that this scenario is consistent with many diverse tunneling observations give us much confidence on it being at least close to the truth.

ACKNOWLEDGMENTS

We thank Dr. J. C. Seamus Davis and Ms. Kristine Lang for providing us quantitative information about the measurement they published in their recent Nature article.[28] This work was supported by the Texas Center for Superconductivity at the University of Houston, the Robert A. Welch Foundation, the Grant under the No. NSF-INT-9724809, and by the Texas Higher Education Coordinating Board under grant No. 1997-010366-029.

[1] C.-R. Hu, Phys. Rev. Lett. **72**, 1526 (1994); J. Yang and C. R. Hu, Phys. Rev. B **50**, 16766 (1994).

[2] C.-R. Hu, Bull. Amer. Phys. Soc. **40**, 789 (1995); *ibid.*, **41**, 361 (1996); Proc. 10th Anniv. HTS Workshop on Phys. mater. and Appl. ed. B. Batlogg et al. (World Scientific, Singapore, 1996) p. 551.

[3] Y. Tanaka and S. Kashiwaya, Phys. Rev. Lett. **74**, 3451 (1995); Phys. Rev. B **53**, R11957 (1996). Yu. S. Barash, H. Burkhardt, and D. Rainer, Phys. Rev. Lett. **77**, 4070 (1996); Yu. S. Barash, Phys. Rev. B **61**, 678 (2000).

[4] C.-R. Hu, Phys. Rev. B **57**, 1266 (1998).

[5] M. E. Zitomirsky and M. B. Walker, Phys. Rev. Lett. **79**, 1734 (1997); D. L. Feder, A. Bedsall, A. J. Berlinsky, and C. Kallin, Phys. Rev. B **56**, R5751 (1997); W. Belzig, C. Bruder, and M. Sigrist, Phys. Rev. Lett. **80**, 4285 (1998).

[6] The most extensively studied type of experiments involves the observation of a zero-bias conductance peak in single particle tunneling. This type of experiments is reviewed in detail later in this work.

[7] H. Walter, W. Prusseit, R. Semerad, H. Kinder, W. Assmann, H. Huber, H. Burkhardt, D. Reiner, and J. M. Sauls, Phys. Rev. Lett. **80**, 3598 (1998). This work showed that MS's can explain an observed low temperature anomaly in the magnetic penetration depth in ion-irradiated HTSC samples.

[8] X.-Z. Yan and C.-R. Hu, Phys. Rev. Lett. **83**, 1656 (1999). This work showed that MS's can explain the non-Fraunhofer magnetic-field dependence in the Josephson critical current of a {110}|{001} HTSC junction observed by Y. Ishimaru, J. Wen, N. Koshizuka, and Y. Enomoto [Phys. Rev. B **55**, 11851 (1997)].

[9] G. Preosti, H. Kim, and P. Muzikar, Phys. Rev. B **50**, 1259 (1994); R. Fehrenbacher and M. R. Norman, Phys. Rev. B **50**, 3495 (1994).

[10] P.J. Hirschfeld, P. Wölfle, and D. Einzel, Phys. Rev. B **37**, 83 (1988); S. Schmitt-Rink, K. Miyake, and C. M. Varma, Phys. Rev. Lett. **57**, 2575 (1986).
[11] A.V. Balatsky, M.I. Salkola, and A. Rosengren, Phys. Rev. B **51**, 15547 (1995); M. I. Salkola, A. V. Balatsky, and D. J. Scalapino, Phys. Rev. Lett. **77**, 1841 (1996).
[12] L. J. Buchholtz and G. Zwicknagl, Phys. Rev. B **23**, 5788 (1981).
[13] R. Joynt, Physica B **261**, 479 (1999).
[14] T. Xiang and J.M. Wheatley, Phys. Rev. B **51**, 11721 (1995).
[15] Y. Onishi, Y. Ohashi, Y. Shingaki, and K. Miyake, J. Phys. Soc. Jpn. **65**, 675 (1996).
[16] M. Franz, C. Kallin, and A.J. Berlinsky, Phys. Rev. B **54**, R6897 (1996).
[17] P. A. Lee, Phys. Rev. Lett. **71**, 1887 (1993); A. V. Balatsky and M. I. Salkola, Phys. Rev. Lett. **76**, 2386 (1996); D. N. Aristov and A. G. Yashenkin, Phys. Rev. Lett. **80**, 1116 (1998); A. V. Balatsky and M.I. Salkola, Phys. Rev. Lett. **80**, 1117 (1998).
[18] Y. Tanaka and S. Kashiwaya, Phys. Rev. Lett. **74**, 3451 (1995); S. Kashiwaya, Y. Tanaka, M. Koyanagi, H. Takashima, and K. Kajimura, Phys. Rev. B **51**, 1350 (1995).
[19] J. H. Xu, J. H. Miller, and C. S. Ting, Phys. Rev. B **53**, 3604 (1996).
[20] J.-X. Zhu and C. S. Ting, Phys. Rev. B **57**, 3038 (1998).
[21] J.-X. Zhu, B. Friedman, and C. S. Ting, Phys. Rev. B **59**, 3353 (1999).
[22] L. Alff, H. Takashima, S. Kashiwaya, N. Terada, H. Ihara, Y. Tanaka, M. Koyanagi, and K. Kajimura, Phys. Rev. B **55**, 14757 (1997); J. Y. T. Wei, N.-C. Yeh, D. F. Garrigus, and M. Strasik, Phys. Rev. Lett. **81**, 2542 (1998).
[23] M. Covington, M. Aprili, E. Paraoanu, L. H. Greene, F. Xu, J. Zhu, and C. A. Mirkin, Phys. Rev. Lett. **79**, 277 (1997) [for accompanied theoretical discussion, see M. Fogelström, D. Reiner, and J. Sauls, Phys. Rev. Lett. **79**, 281 (1997)]; S. Sinha and K.-W. Ng, Phys. Rev. Lett. **80**, 1296 (1998); M. Aprili, M. Covington, E. Paraoanu, B. Niedermeier, and L. H. Greene, Phys. Rev. B **57**, R8139 (1998); L. Alff, A. Beck, R. Gross, A. Marx, S. Kleefisch, Th. Bauch, H. Sato, M. Naito, and G. Koren, Phys. Rev. B **58**, 11197 (1998); L. Alff, S. Kleefisch, U. Schoop, M. Zittartz, T. Kemen, T. Bauch, A. Marx, and R. Gross, Eur. Phys. J. B **5**, 423 (1998); M. Aprili, E. Badica, and L. H. Greene, Phys. Rev. Lett. **83**, 4630 (1999); R. Krupke and G. Deutscher, *ibid.*, 4634; W. Wang et al., Phys. Rev. B **60**, 4272 (1999).
[24] G.E. Blonder, M. Tinkham, and T.M. Klapwijk, Phys. Rev. B **25**, 4515 (1982).
[25] Y. Tanuma, Y. Tanaka, M. Yamashiro, and S. Kashiwaya, Phys. Rev. **57**, 7997 (1998). This theoretical work found a zero-energy peak in the *local* DOS at certain isolated sites near a non-flat {100} surface. It is not clear whether this feature has enough spectral weight to be observable in non-STM/S types of tunneling.
[26] A. Yazdani, C. M. Howald, C. P. Lutz, A. Kapitulnik, and D. M. Eigler, Phys. Rev. Lett. **83**, 176 (1999).
[27] E. W. Hudson, S. H. Pan, A. K. Gupta, K.-W. Ng, and J. C. Davis, Science **285**, 88 (1999).
[28] S. H. Pan, E. W. Hudson, K. M. Lang, H. Eisaki, S. Uchida, and J. C. Davis, Nature **403**, 746 (2000); See also, cond-mat/9909365.
[29] P. Romano, A.M. Cucolo, R. Di Leo, E. Bacca, and P. Prieto, Physica C **296**, 210 (1998); A.M. Cucolo, R. Di Leo, A. Nigro, P. Romano, E. Bacca, W. Lopera, M.E. Gomez, and P. Prieto, IEEE Trans. Appl. Supercond. **7**, 2848 (1997); H.Z. Durusoy, D. Lew, L. Lombardo, A. Kapitulnik, T.H. Geballe, and M.R. Beasley, Physica C **266**, 253 (1996); D. Mandrus, L. Forro, D. Koller, and L. Mihaly, Nature **351**, 460 (1991).
[30] A.M. Cucolo, R. Di Leo, A. Nigro, P. Romano, F. Bobba, E. Bacca, and P. Prieto, Phys. Rev. Lett. **76**, 1920 (1996).
[31] M. Taira, M. Suzuki, X.-G. Zheng, and T. Hoshino, J. Phys. Soc. Jpn. **67**, 1732 (1998); H.J. Tao, F. Lu, E.L. Wolf, Physica C **282 - 287**, 1507 (1997).
[32] J. Lesueur, L.H Greene, W.L. Feldmann, and A. Inam, Physica C **191**, 325 (1992); M. Gurvitch, J.M. Valles, Jr., A.M. Cucolo, R.C. Dynes, J.P. Garno, L.F. Schneemeyer, and J.V. Waszczak, Phys. Rev. Lett. **63**, 1008 (1989).
[33] H. Hancotte, R. Deltour, D.N. Davydov, A.G.M. Jansen, and P. Wyder, Physica C **282-287**, 1487 (1997).
[34] H. Tsuchiura, Y. Tanaka, M. Ogata, and S. Kashiwaya, J. Phys. Soc. Jpn. **68**, 2510 (1999); Phys. Rev. Lett. **84**, 3165 (2000).
[35] J.-X. Zhu, T. K. Lee, C. S. Ting, and C.-R. Hu, Phys. Rev. B **61**, 8667 (2000); See also, cond-mat/9909363.
[36] P. G. de Gennes, *Superconductivity of Metals and Alloys* (Benjamin, New York, 1966).
[37] M. Tinkham, *Introduction to Superconductivity* (McGraw Hill, New York, 1975).
[38] The two resonant states for each spin have energies symmetrically placed around zero energy — one positive and one negative. The negative-energy state is related to the positive-energy state by the transformation $\epsilon \to -\epsilon$, $u_{\mathbf{j}} \to v_{\mathbf{j}}$, and $v_{\mathbf{j}} \to -u_{\mathbf{j}}$. The positive-energy resonant state is found to have the symmetry property that u has $d_{x^2-y^2}$ symmetry, whereas v has extended-s symmetry. Both u and v also show oscillation at essentially the Fermi wavelength as well as a decay in roughly the radial direction. These properties, plus the fact that both u and v vanish at the origin, can qualitatively account for the magnitude variations of the calculated bare local DTC plotted in Figs. 6 (a) and (b).
[39] B. G. Levi, Phys. Today **53**, 17 (March issue, 2000).

TABLE I. The values of d-wave order parameter and coherence length for several sets of parameter values. The temperature is at $T = 0.02t$.

μ/t	g_1/t	Δ_d/t	ξ_0/a
0	2	0.241	1.33
-0.4	2	0.229	1.32
-0.4	1.5	0.139	2.17
-1	2	0.164	1.68

TABLE II. Comparison between the measured STM/S local differential tunneling conductance at the near-zero-bias resonant energy by Pan *et al.*[28] at the Zn impurity site (00), the nearest neighbor sites (10) and (01), the next nearest neighbor site (11), and the third nearest neighbor sites (20) and (02), (the first row), and the calculated values for the local differential tunneling conductance at zero bias at the same sites before the transformation (according to Eq. (7)) (the second row), and after the transformation (the third row). The data in each row is normalized so that the largest value is unity, which occurs at the (00) site in the first and the third rows, but at the (10) and (01) sites in the second row.

(00)	(10) & (01)	(11)	(20) & (02)
1.00	0.18	0.29	0.13
0.000	1.000	0.078	0.113
1.000	0.068	0.593	0.384

FIG. 1. The local differential tunneling conductance as a function of a bias at the site directly on the site (18,18) (a) and (19,18) (b) in a DWSC with each supercell containing one single impurity located at site (18,18). The impurity strength $U_0 = 2.5t$ (solid line) and $10t$ (dashed line). The other parameters $\mu = 0$ and $g_1 = 2t$.

FIG. 2. The local differential tunneling conductance as a function of bias in a DWSC with each supercell containing one single impurity located at site (18,18) for $\mu = 0$ (solid line), $-0.4t$ (dashed line), and $-t$ (short-dashed line). The parameter value of g_1 is taken to be $2t$. The measure point is at (19,18).

FIG. 3. The local differential tunneling conductance as a function of bias in a d-wave superconductor with each supercell containing one single impurity (solid line) at site (18,18), and two (dashed line) at sites (17,19) and (18,18), and three impurities (short-dashed line) at sites (17,19), (18,18) and (19,17) aligned consecutively along the {110} direction. The parameters $g_1 = 2t$ and $\mu = -t$. The measure point is at site (19,18).

FIG. 4. The lowest positive eigenvalue as a function of the distance between two impurities aligned along the {110} direction in the CuO_2 plane. The parameters $g_1 = 2t$ and $\mu = -t$.

FIG. 5. The number of near-zero energy states versus the number of impurities aligned consecutively along the {110} direction in the CuO_2. The parameters $g_1 = 2t$ and $\mu = -t$.

FIG. 6. Spatial distribution of the differential tunneling conductance at zero bias: The three-dimensional display in the whole supercell before summation over four nearest-neighboring Cu sites (a) and the corresponding two-dimensional bubble view in a small region near the impurity (b); the three-dimensional display after summation (c) and the corresponding two-dimensional bubble view (d). The bubble size on each Cu site represents the conductance magnitude. The parameters $g_1 = 1.5t$ and $\mu = -0.4t$.

FIG. 7. The spatially-averaged differential tunneling conductance as a function of bias in a d-wave superconductor with each supercell containing one single impurity [i.e., the impurity concentration c is about 0.08%] (solid line), a random distribution of impurities with $c = 1.28\%$ (dashed line), and 62.5% of the randomly-distributed impurities of the former case changed to diagonal dimers (short-dashed line). The parameters $g_1 = 2t$ and $\mu = -t$.

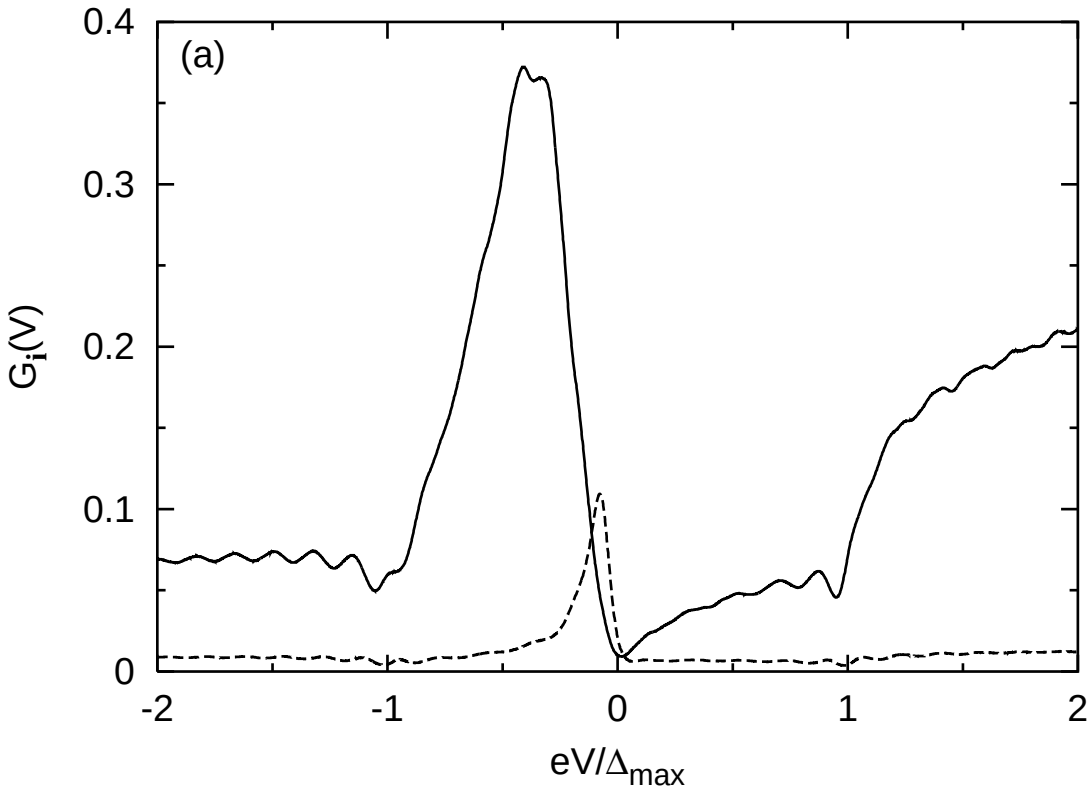

FIG. 1(a) Zhu et al.

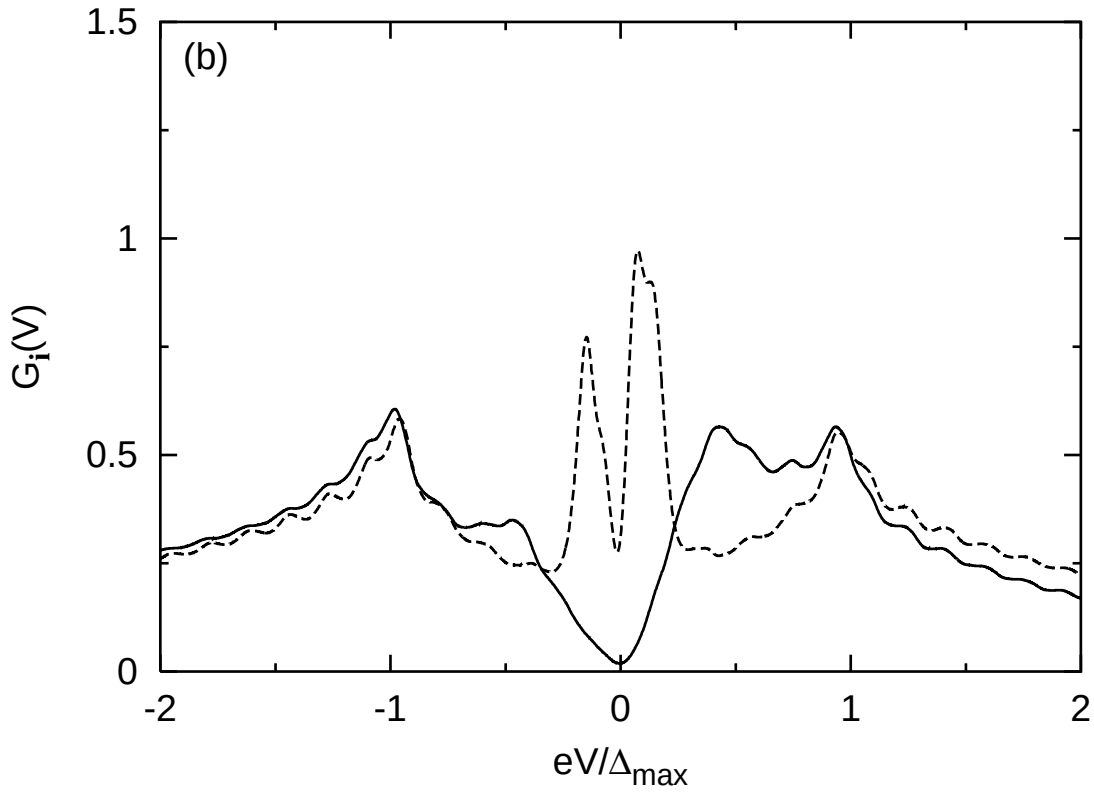

FIG. 1(b) Zhu et al.

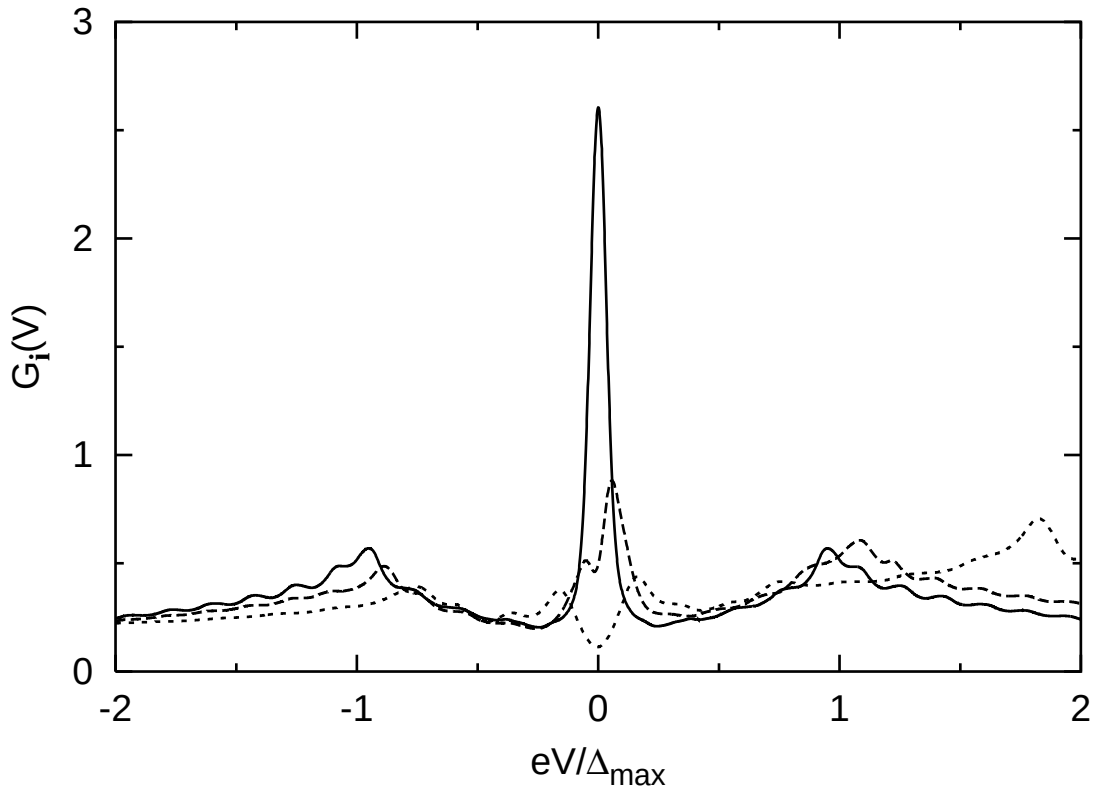

FIG. 2 Zhu et al.

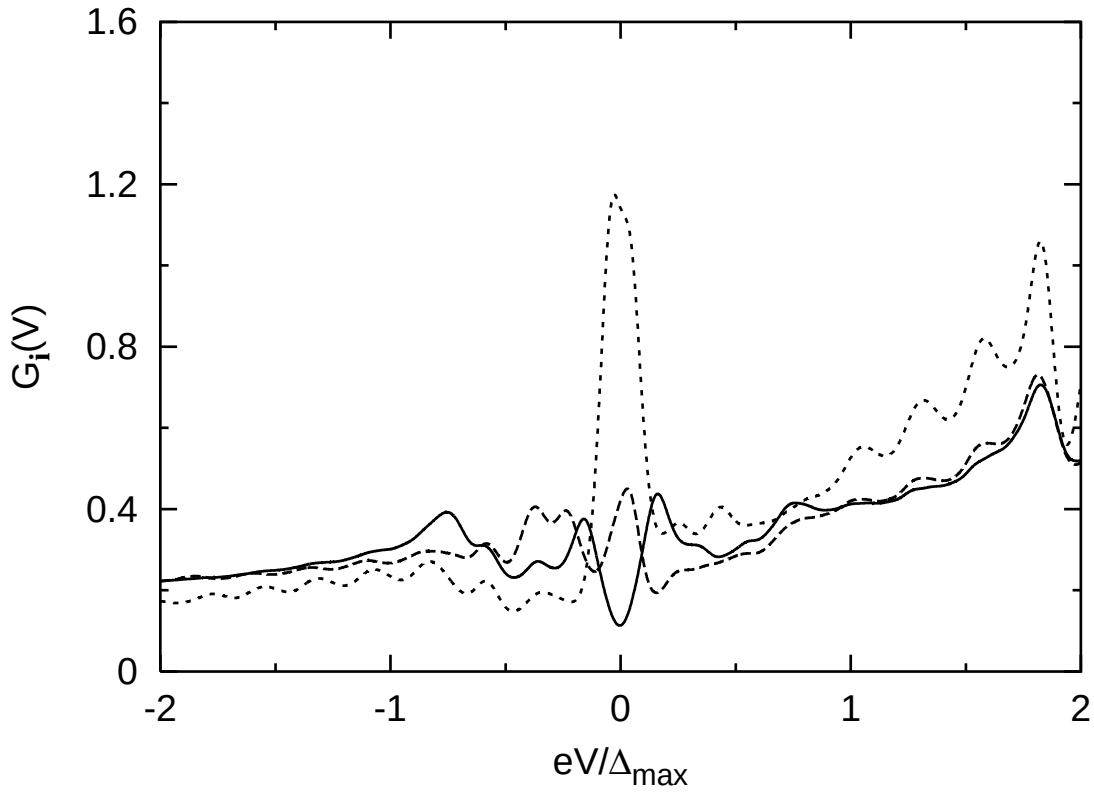

FIG. 3 Zhu et al.

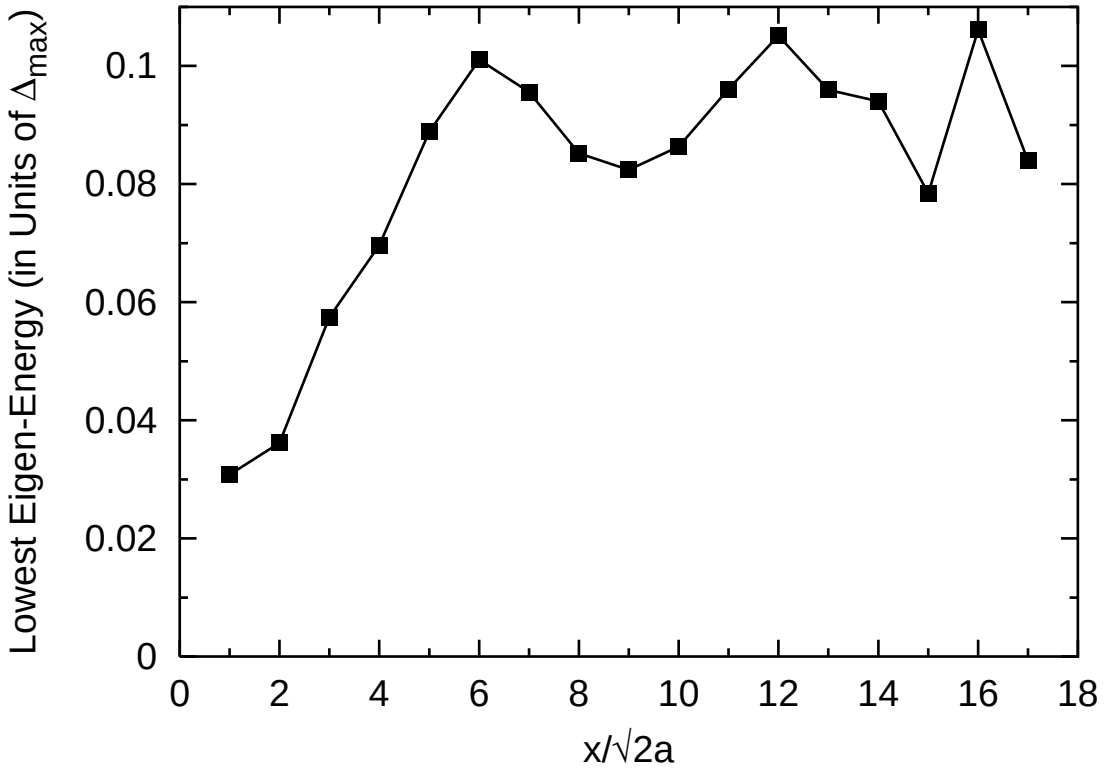

FIG. 4 Zhu et al.

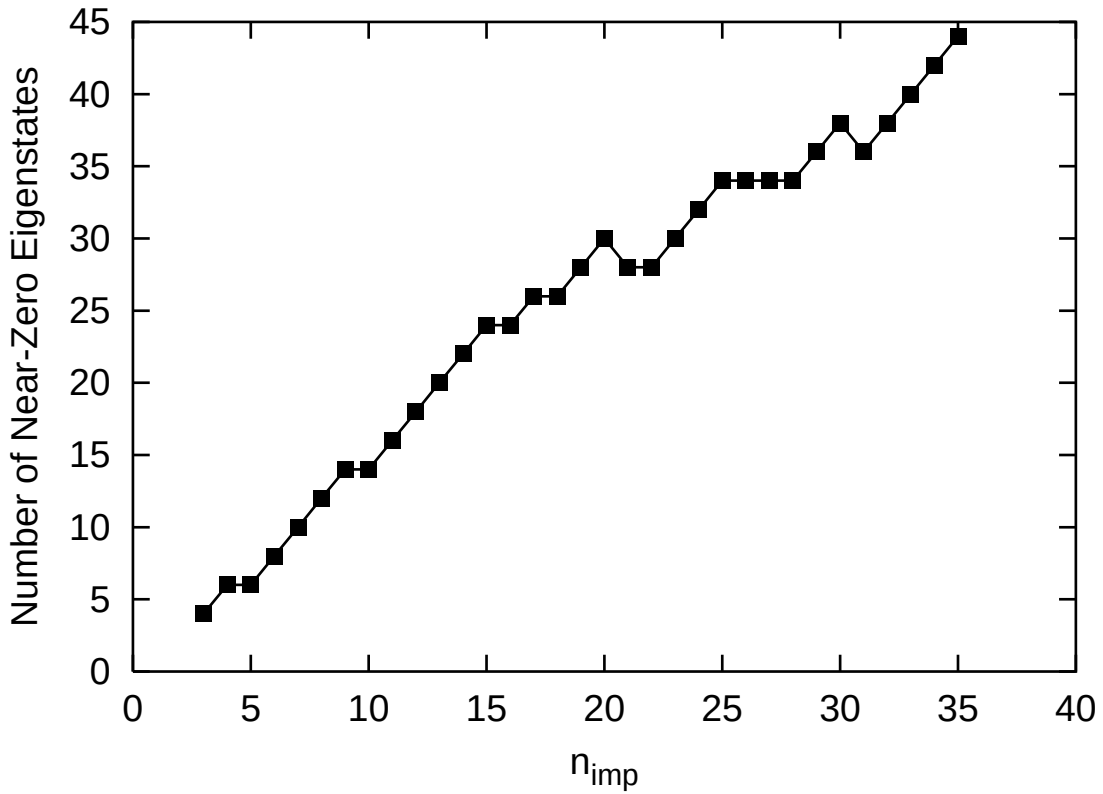

FIG. 5 Zhu et al.

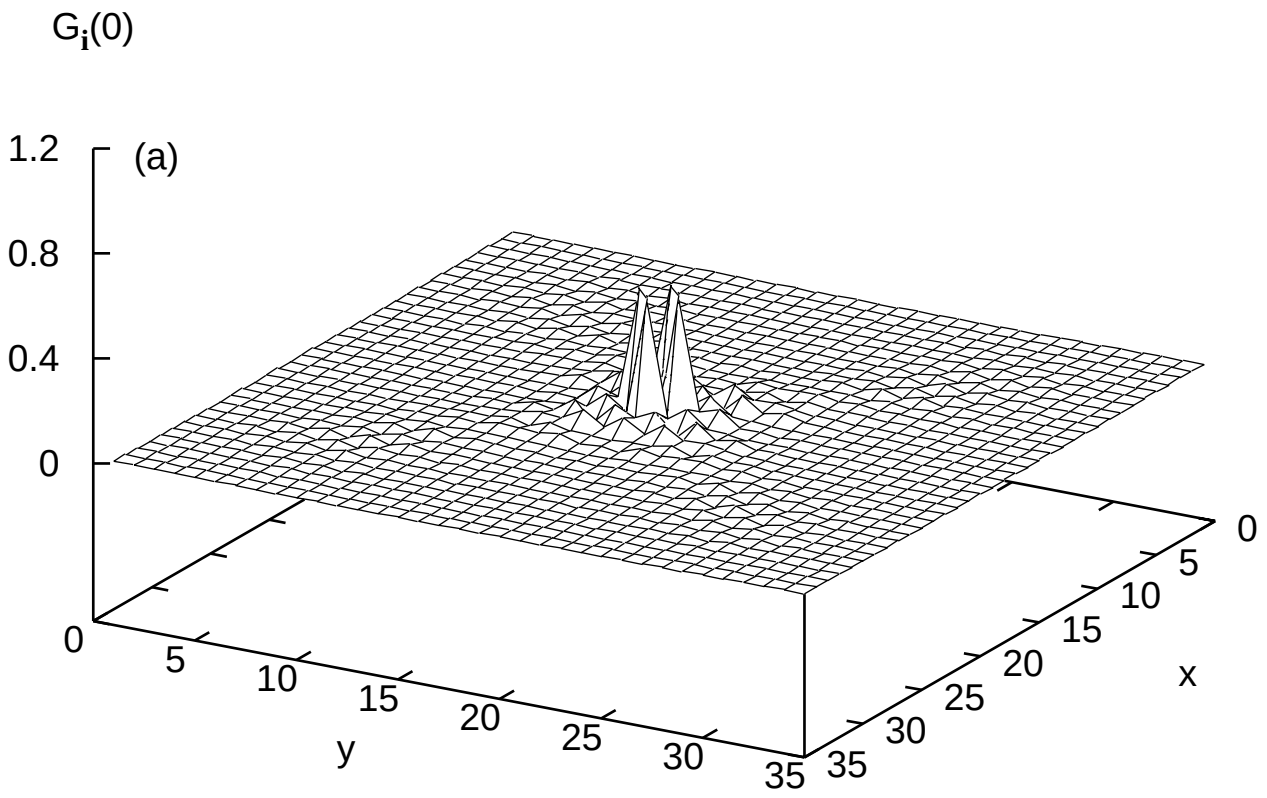

FIG. 6(a) Zhu et al.

FIG. 6(b) Zhu et al.

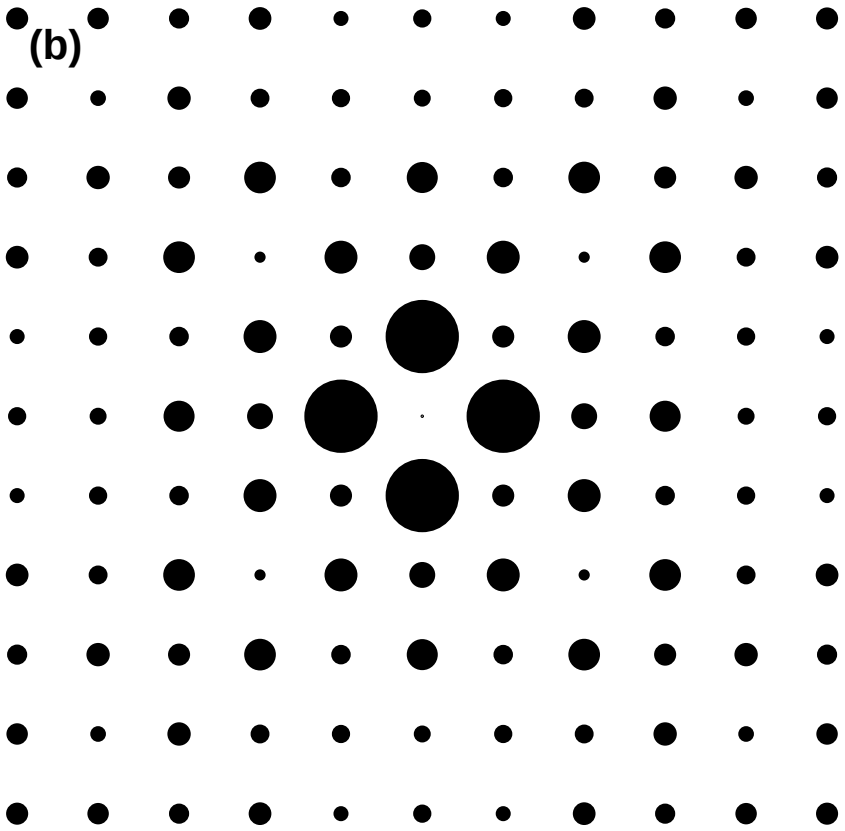

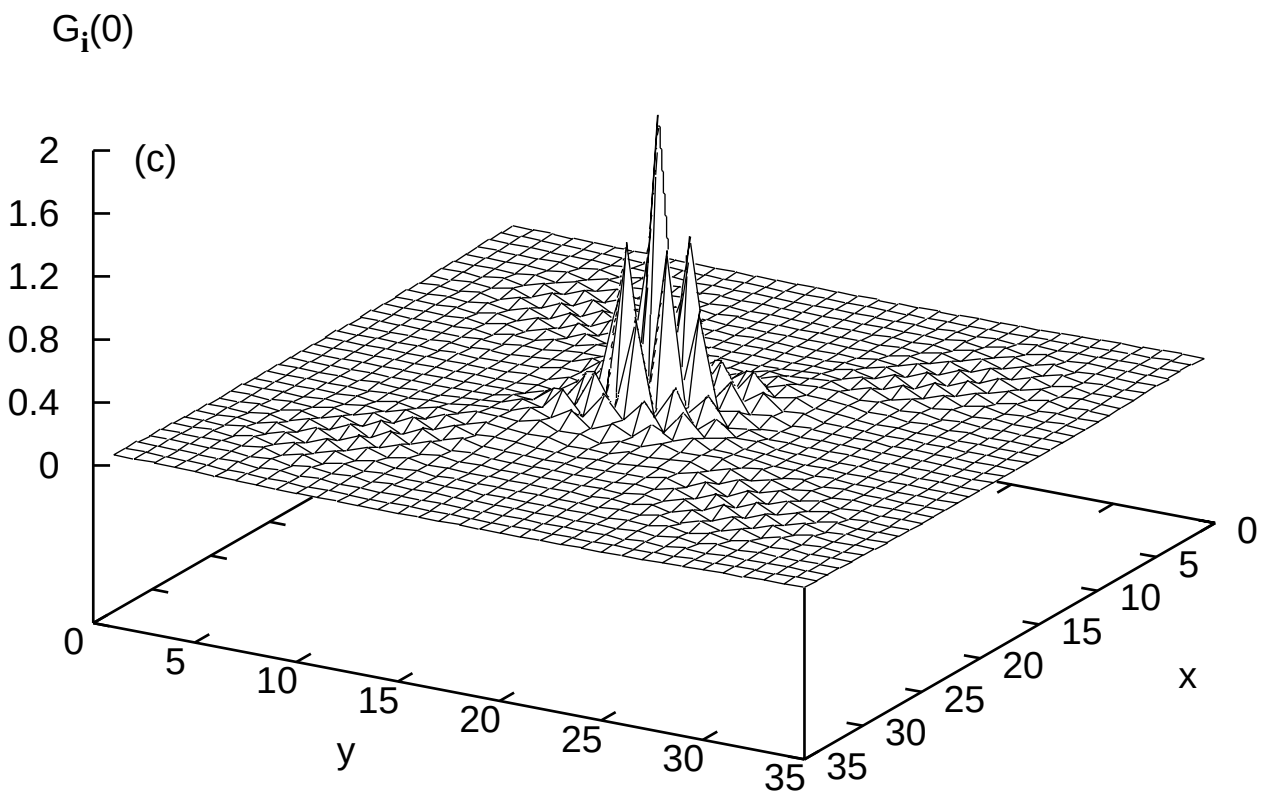

FIG. 6(c) Zhu et al.

FIG. 6(d) Zhu et al.

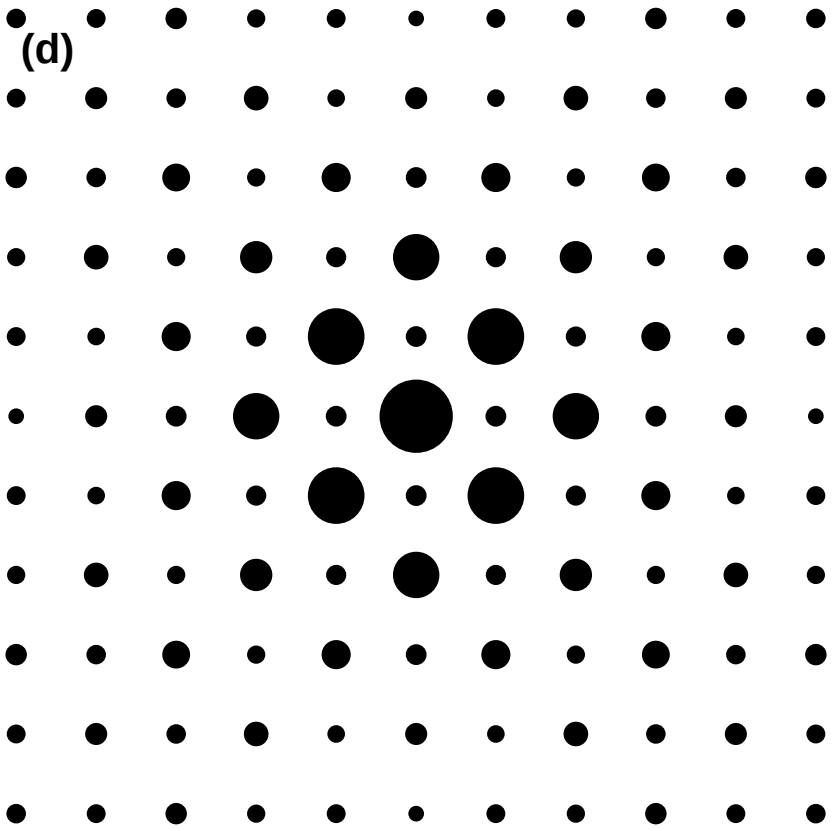

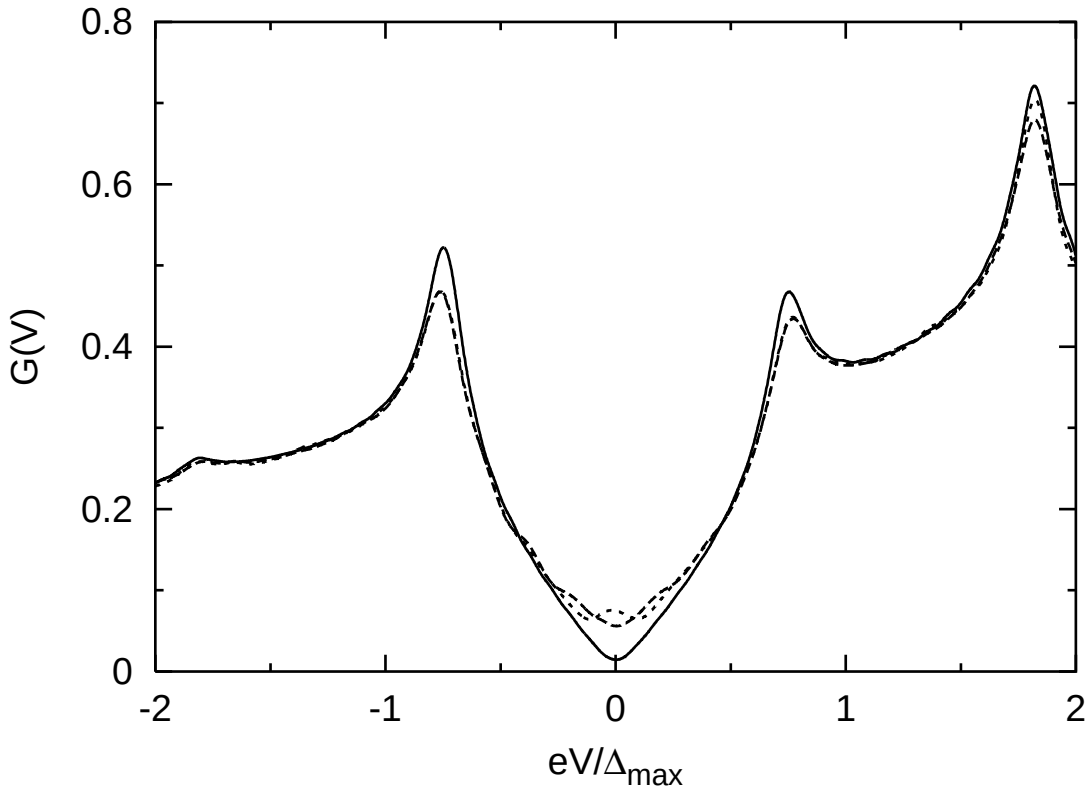

FIG. 7 Zhu et al.